BRL MR 2214

BRL

MEMORANDUM REPORT NO. 2214

THE SHOCK HUGONIOT OF MINERAL OIL

by

P. Netherwood
D. Tauber

August 1972

U.S. ARMY ABERDEEN RESEARCH AND DEVELOPMENT CENTER
BALLISTIC RESEARCH LABORATORIES
ABERDEEN PROVING GROUND, MARYLAND

Destroy this report when it is no longer needed.
Do not return it to the originator.

Secondary distribution of this report by originating or sponsoring activity is prohibited.

Additional copies of this report may be purchased from the U.S. Department of Commerce, National Technical Information Service, Springfield, Virginia 22151

The findings in this report are not to be construed as an official Department of the Army position, unless so designated by other authorized documents.

The use of trade names or manufacturers' names in this report does not constitute indorsement of any commercial product.

B A L L I S T I C R E S E A R C H L A B O R A T O R I E S

MEMORANDUM REPORT NO. 2214

AUGUST 1972

THE SHOCK HUGONIOT OF MINERAL OIL

P. Netherwood
D. Tauber

Terminal Ballistics Laboratory

RDT&E Project No. 1T061102311A

A B E R D E E N P R O V I N G G R O U N D, M A R Y L A N D

B A L L I S T I C R E S E A R C H L A B O R A T O R I E S

MEMORANDUM REPORT NO. 2214

PHNetherwood/DTauber/erf
Aberdeen Proving Ground, Md.
August 1972

THE SHOCK HUGONIOT OF MINERAL OIL

ABSTRACT

The shock Hugoniot of heavy mineral oil (density = 0.87g/cc) has been determined by plane shock wave experiments. A charged capacitor technique was used to measure shock velocities through specimens of mineral oil. Shock velocities through polymethyl methacrylate reference specimens were measured by a shock-induced polarization technique, and impedance calculations were performed to establish the Hugoniot equation of state in mineral oil. Within the pressure range from 15 to 150 kilobars, the Hugoniot curve of heavy mineral oil was found to be represented by the linear relationship $U=2.19 + 1.52u$, where U is shock velocity, u is particle velocity, and velocity units are mm/μsec.

TABLE OF CONTENTS

LIST OF ILLUSTRATIONS

LIST OF SYMBOLS

c	rarefaction velocity, mm/μsec
c^*	approximate rarefaction velocity, mm/μsec
k	relative dielectric constant of the shock compressed dielectric
k_o	relative dielectric constant at zero pressure
r	shock curvature near a lateral boundary, mm
r^*	approximate curvature, mm
t	time, μsec
t_o	time of shock entry into sample, μsec
t_1	time at end of initial signal rise, μsec
t_2	time of shock arrival at second electrode, μsec
Δt	risetime of signal, t_1-t_0, μsec
u	particle velocity, mm/μsec
w	sample diameter, mm
x_o	sample thickness, mm
A	electrode area, cm^2
P	pressure, kilobars
T	transit time, corrected, μsec
U	shock velocity, mm/μsec
V	applied voltage, V
ε_o	permittivity of free space, 8.854×10^{-2} F/m
ρ	density of the shock compressed material, g/cc
ρ_o	initial density of the material, g/cc
σ	standard deviation of the mean, shock velocity, mm/μsec

I. INTRODUCTION

Mineral oil has been used in shock wave experiments to eliminate electrically noisy air shock.[1*] It is particularly well suited to this application because it produces a very small shock-induced electrical signal,[2] and therefore does not contribute to other electrical signals. The Ballistic Research Laboratories have also used heavy mineral oil (HMO)[3] to improve impedance matching at interfaces, and as a shock transmitting medium. In the latter application, the Hugoniot of HMO was needed to establish shock pressures.

The Hugoniot of HMO was determined using the impedance match technique.[4] In this technique, specimens of HMO and polymethyl methacrylate (PMMA)[5] were placed on a metal plate through which an explosively produced plane shock wave was transmitted. Transit times of shock waves through the PMMA reference specimens were measured from the shock-induced polarization signal[6] and used to calculate the average shock velocities. The polarization signal from HMO is very small, so a charged-capacitor technique[7] was used to measure the shock-wave transit times from which average shock velocities were calculated. Hugoniot points for HMO were then obtained by impedance calculations. This report describes the experimental details and presents the Hugoniot data obtained for HMO.

II. EXPERIMENTAL TECHNIQUES

A. Shock Pressures

Plane shock waves were generated by the explosive train shown schematically in Figure 1. This explosive train consisted of a 10-cm diameter composition B-TNT plane wave lens and a 10-cm diameter by 2.5-cm thick base charge of TNT, composition B, or 75/25 Octol. The plane shock wave from the explosive was transmitted to the test specimens through a buffer plate. The higher shock pressures were produced by using different base charges on 0.6-cm thick buffer plates of AZ31B magnesium, 2024 aluminum, or A.S.T.M. B16 brass. The low shock pressures

*References are found on page 25

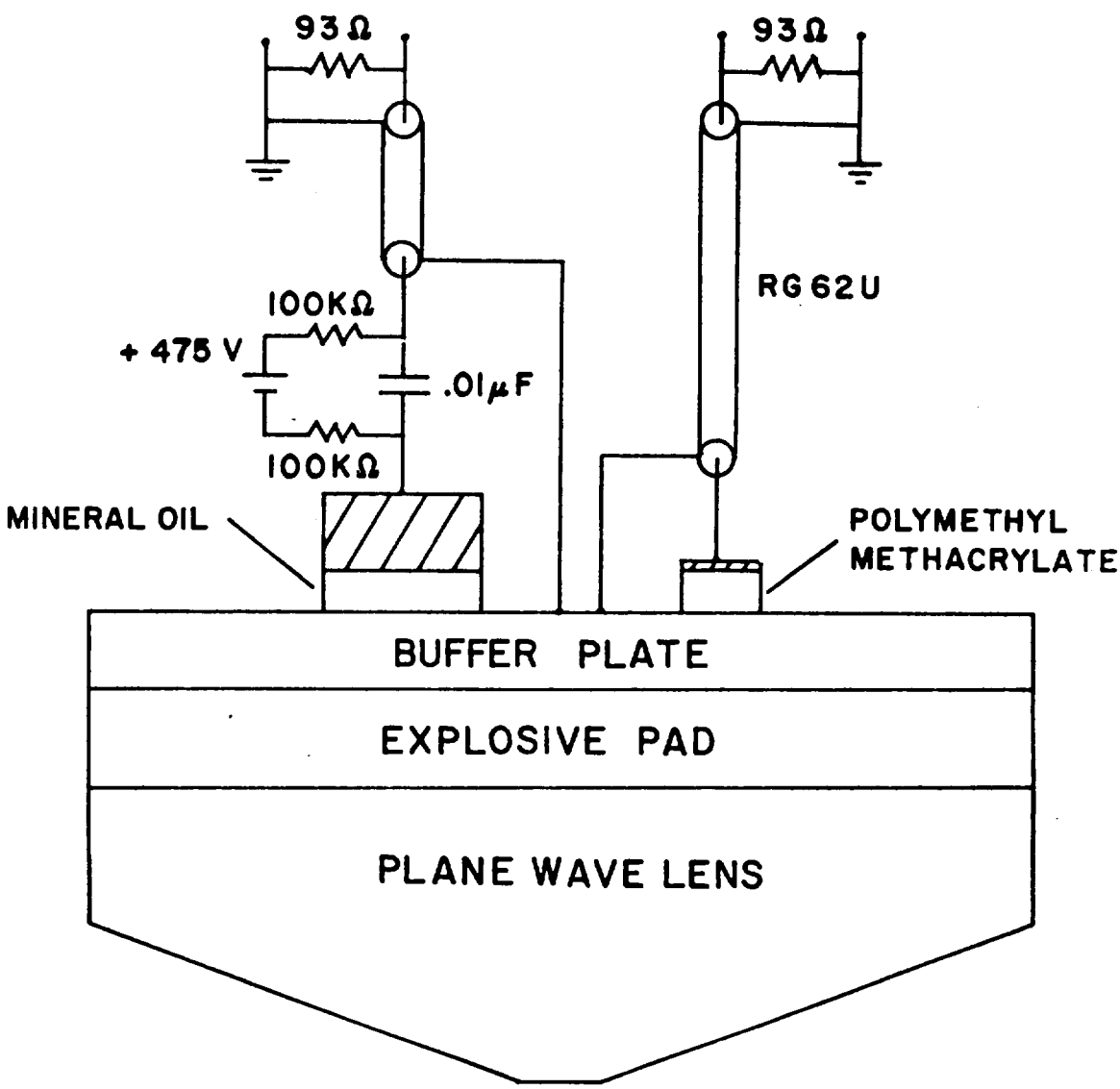

Figure 1. Experimental Arrangement for Simultaneous Measurement of Shock Velocities in Mineral Oil and Polymethyl Methacrylate

were produced by using a TNT base charge on a laminated buffer which reduced the pressures by impedance mismatch between laminations. The laminated buffer consisted of three 0.6cm thick laminations, brass-x-brass, where x was low density polyethylene or AZ31B magnesium.

These systems produce shock waves which are plane to 0.1 microseconds over diameters of two to three and one-half inches. Each experiment is designed to use only the plane portion of the wave. The plane wave is delivered normally incident to the buffer-sample interface. In practice some of the waves will arrive with measurable obliquity. This is assessed and compensated for by measurements of signal risetime, as described in Section III.

B. Experimental Arrangement for Mineral Oil Measurements

Shock velocity through mineral oil was measured by a charged capacitor technique. The test capacitor shown in Figure 2 consisted of a 1.27-cm diameter brass second electrode suspended 0.10-cm from the buffer plate which served as the first electrode. The HMO sample was introduced into the interelectrode gap and was retained by capillary action. The test capacitor was charged to a potential of 475 volts. A 0.01 microfarad capacitor, in parallel with the test capacitor, held the applied voltage essentially constant during an experiment. The test capacitor was connected in series with a coaxial cable terminated by its characteristic impedance at the input of a fast rise oscilloscope.[8] Under static conditions, no current flowed in the circuit after the capacitor was initially charged. When the explosive charge was detonated, a plane shock wave passed through the buffer plate and entered the HMO, compressing it and increasing the dielectric constant. This increased the capacitance of the test capacitor and caused a charging current to flow in the circuit. The resulting voltage drop across the terminating resistor was recorded with an oscilloscope.

As shown in Reference 7, the signal profile may be calculated using the equation

$$I = \frac{V\varepsilon_0 k_0 A[U-(k_0/k)(U-u)]}{\{X_0-[U-(k_0/k)(U-u)]t\}^2} \qquad (1)$$

where V is the applied voltage, ε_0 is the permittivity of free space (8.854×10^{-12} F/m), A is the area, k_0 is the relative dielectric constant at zero pressure, k is the relative dielectric constant of the shock compressed dielectric, x_0 is the initial thickness, and t is the time measured from the entry of the shock front into the dielectric. The dielectric constant under shock compression may be roughly estimated by the Clausius-Mosotti equation, assuming constant polarizability. The Clausius-Mosotti equation was used instead of the Drude equation, which Hauver (7) has shown to be more appropriate for polyethylene, because it predicts a larger change in dielectric constant and therefore a larger signal. This increases the safety factor in the estimate of signal size used to set the oscilloscope and reduces the chance of an off-screen signal. It should be noted that the calculation assumes a three-electrode parallel plate capacitor. The simple, unguarded capacitor design used in these experiments is not suitable for quantitative measurements of the dielectric constant under shock compression, since it provides no protection from edge effects. Nevertheless, the calculation provides a rough estimate of signal size, and the unguarded design does provide signals which may be readily interpreted and measured for shock transit time, which is the only value needed for the Hugoniot measurement.

C. Experimental Arrangement for Polymethyl Methacrylate Measurements

The shock velocity through the PMMA[5] reference specimens was measured by a shock-induced polarization technique.[6] The experimental arrangement is shown in Figure 3. A PMMA specimen, 0.72cm in diameter by 0.10cm thick, was placed in contact with the buffer plate which served as the first electrode. The other surface of the PMMA specimen was covered with a spring-loaded brass disc which served as the second electrode. A grounded aluminum ring was used as electrical shielding. The electrodes were connected to an oscilloscope by a coaxial cable which was terminated with its characteristic impedance at the oscilloscope input. When the

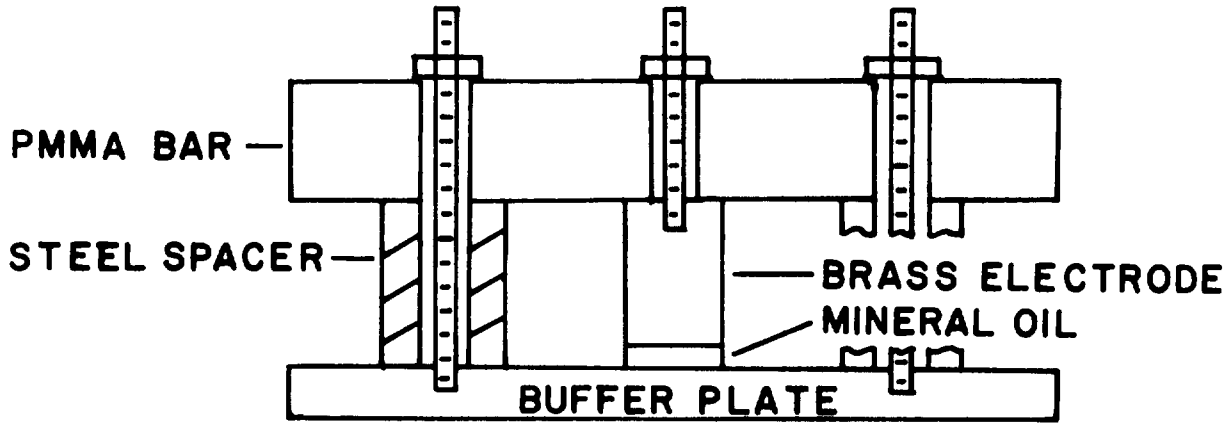

Figure 2. Mineral Oil Capacitor

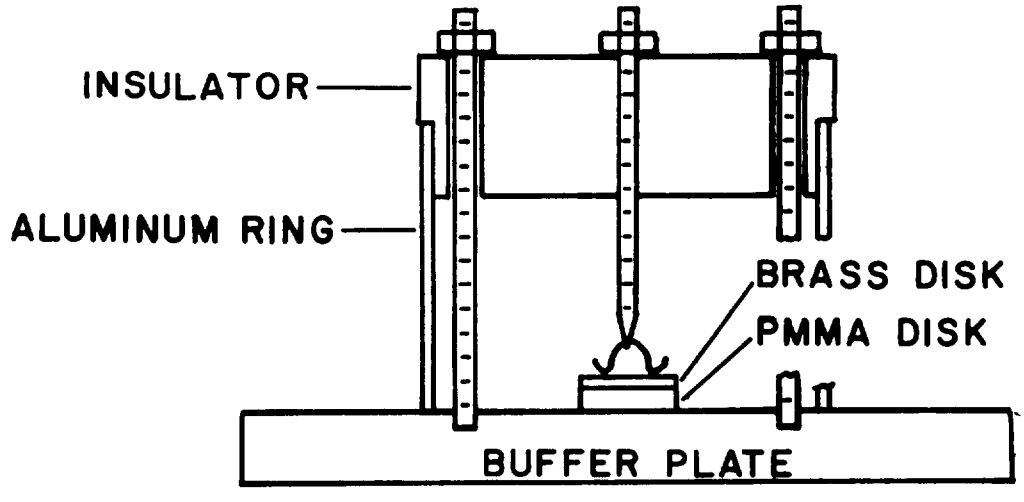

Figure 3. Polymethyl Methacrylate Shock-Induced Polarization Transducer

plane shock wave entered the PMMA specimen from the first electrode, polarization was induced and a displacement current charged the capacitance in the circuit. The voltage drop across the cable termination was displayed on the oscilloscope. The shock transit time was obtained from the duration of the polarization and was used to calculate the average shock velocity.

III. SIGNAL MEASUREMENT AND ANALYSIS

Typical signals from HMO and PMMA are shown in Figure 4. Despite the difference in the generating mechanism, the two types of signals appear similar and were measured the same way.

A sharp initial voltage rise occurred at time t_0 when the shock wave entered the specimen. The risetime t_1-t_0 resulted from tilt and/or curvature of the incident shock front. After time t_1, the signal profile increased slowly until time t_2, when the shock wave arrived at the second electrode. The apparent transit time t_2-t_0 was corrected for risetime, and was used with the measured thickness to calculate the average shock velocity through the specimen. Since the shock wave undergoes attenuation as it passes through the samples, the calculated velocity will be slightly lower than that at the buffer-sample interface. The HMO and PMMA samples are the same thickness and the shock waves in both samples will be attenuated by comparable amounts. The net effect will be to shift the measured point a short distance down the U_s-u_p curve. The attenuation in PMMA has been shown (reference 6) to be about 0.5%/mm. The design of the experiment therefore assures that any error from this source is very small.

A risetime correction is necessary when the shock front is obliquely incident. Because of pressure release at the free lateral boundary of the specimen, times t_0 and t_2 relate to shock paths that originate from different points along the incident shock front, necessitating a correction to t_2-t_0. An obliquely incident shock front is considered to be

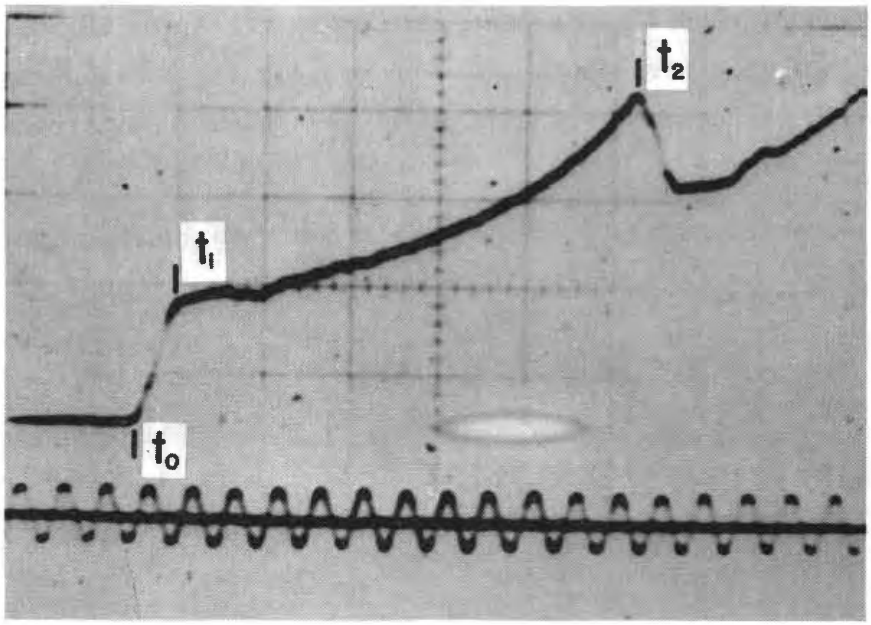

Figure 4a. Mineral Oil Change of Dielectric Constant Signal. Vertical scale 0.2 volts/div, horizontal scale 0.04 μsec/div, timing marks 0.020 μsec intervals.

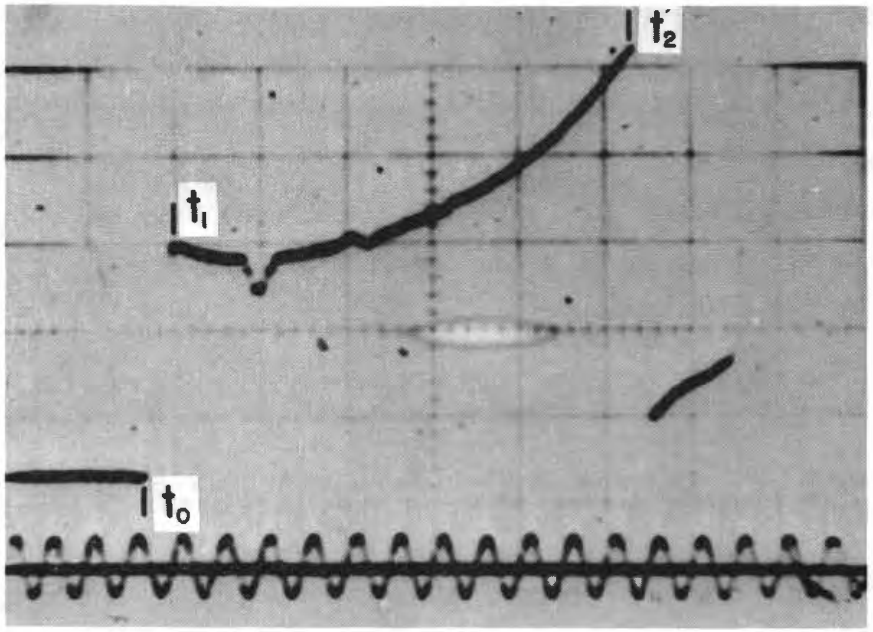

Figure 4b. Polymethyl Methacrylate Shock-Induced Polarization Signal. Vertical scale 0.2 volts/div, horizontal scale 0.04 μsec/div timing marks 0.02 μsec intervals.

the more general condition encountered, so the risetime correction is always applied when the signal risetime exceeds the oscilloscope risetime. The RC response of the circuit is less than the instrument risetime.

The corrected transit time for a plane but obliquely incident shock wave has been shown to be (see Reference 6).

$$T = (t_2 - t_0) - \Delta t(\frac{r}{w}) \tag{2}$$

where T is corrected transit time, $\Delta t = t_1 - t_0$, w is the diameter of the sample and r is the curvature (the radial distance from the edge of the sample to the point where the shock wave first strikes the rear electrode).

The curvature, r, for PMMA has been measured[6] and may be applied directly. The curvature for HMO has not been measured and was estimated. This was done by first calculating uncorrected values for the Hugoniot equation in the form U =a+bu, where a and b are constants. The approximate sound velocity, c, of the lateral release wave at each experimental pressure was then calculated using Jacobs' approximation[9]

$$c \simeq \frac{U-u}{U}(U-bu) \quad . \tag{3}$$

The approximate curvature, r^*, was then calculated from the geometric relationship of the compression and lateral release waves. As shown in reference 6, the true sound velocity is given by

$$c = U[(\frac{r}{x_0})^2 + (\frac{\rho_0}{\rho})^2]^{1/2}$$

where c is the sound velocity and x_0 is the initial thickness of the HMO specimen. This equation may be written

$$c = U[(\frac{r}{x_0})^2 + (\frac{U-u}{U})^2]^{1/2}$$

or, solving for r,

$$r = x_0\left[\left(\frac{c}{u}\right)^2 - \left(\frac{U-u}{U}\right)^2\right]^{1/2}$$

Since the value calculated for c by Jacobs equation is an approximation, c^*, the value calculated for the curvature r, will be r^*, the approximate curvature

$$r^* = x_0\left[\left(\frac{c^*}{u}\right)^2 - \left(\frac{U-u}{U}\right)^2\right]^{1/2} \quad . \tag{4}$$

The approximate curvature for the mineral oil was used in Equation (2) to calculate corrected transit times and shock velocities for HMO. The corrections were small $\left[\Delta t \left(\frac{r}{w}\right) \leq 1\%(t_2 - t_0)\right]$ so the approximations involved do not greatly affect the results.

The Hugoniots of PMMA and the buffer plate metals are well established in the pressure ranges studied here.[10] The pressure and particle velocity in the PMMA were calculated from the shock velocity, using the relationship $U = 2.695 + 1.538u$, and the conservation relation $P = \rho_0 Uu$.

The method of impedance matching was used to determine the buffer plate conditions. The release adiabat of the buffer material must pass through the previously determined PMMA point. This locates the buffer pressure and particle velocity point and identifies the locus of states which can be attained in a material in contact with the buffer plate. The reflected buffer Hugoniot was used as an approximation for the buffer adiabat. Since the PMMA and HMO Hugoniots are in close proximity, this is a good approximation. The HMO Hugoniot point is found at the intersection of the reflected buffer Hugoniot and a line of slope $\rho_0 U$ (mineral oil), where ρ_0 is the initial density of the HMO.

The major sources of error in the experiments reside in the physical measurements of the set-up components (estimated at ±1%). in the measurements of the film records of the oscilloscope traces (estimated at ±1%). the effects of shock wave attenuation (estimated to be less than 0.5%) and the time error due to shock wave obliquity, which is estimated to be less than 2%.

IV. RESULTS

The experimental data are given in Table I and are shown graphically in Figure 5. A linear least squares fit of the data gives the relationship $U = 2.18 + 1.53u$, $\sigma = .076$. A Hugoniot data table based upon this equation is given in Table II.

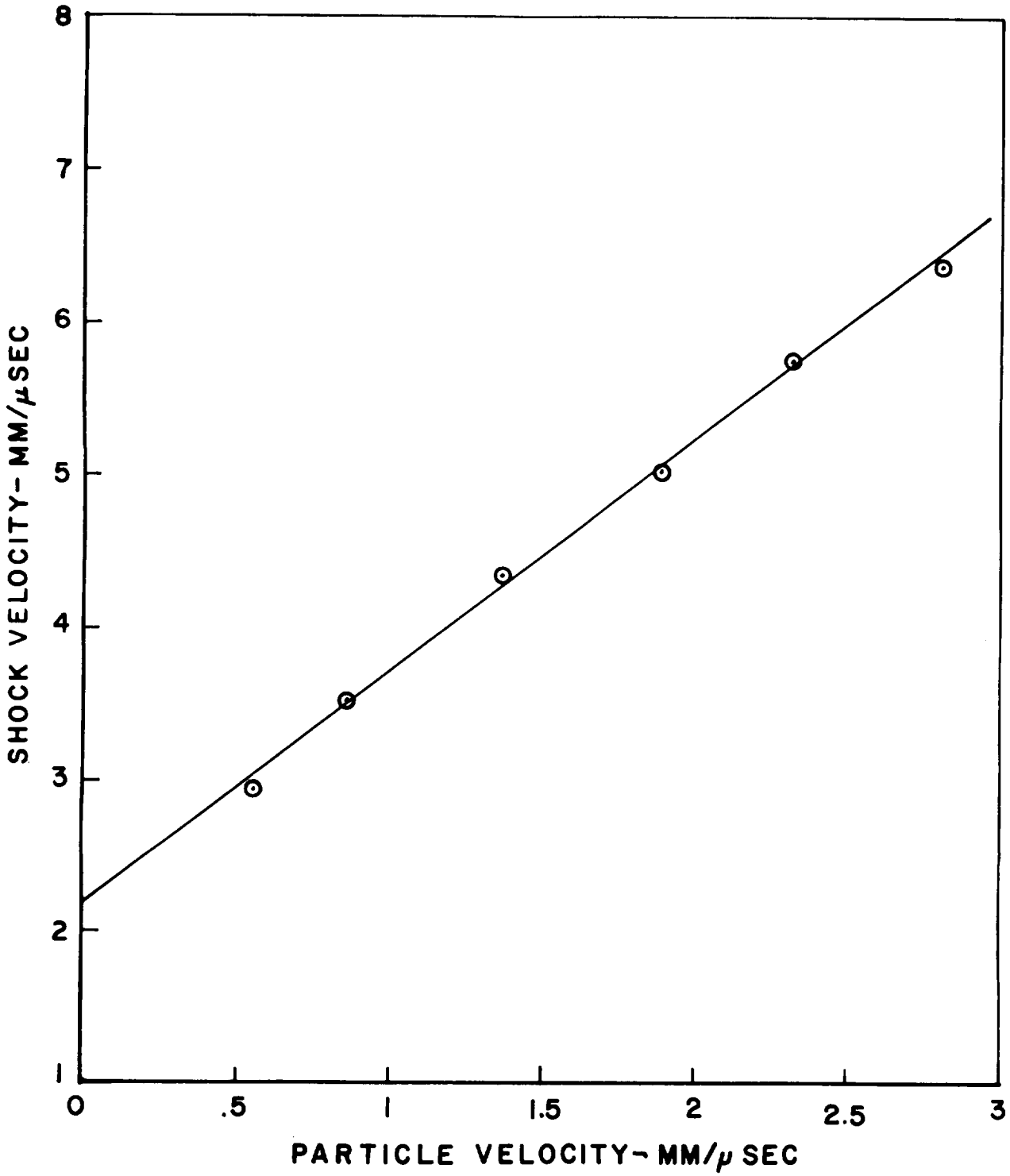

Figure 5. Hugoniot Data for Heavy Mineral Oil, Presented in the Shock Velocity-Particle Velocity Plane.

TABLE I. Experimental Data for Shock Velocity and Particle Velocity in Heavy Mineral Oil

x_0	t_2-t_0	t_2-t_0	U	u
mm	μsec	corrected μsec	mm/μsec	mm/μsec
0.960	0.327	0.326	2.94	0.55
0.945	0.270	0.269	3.51	0.86
0.986	0.227	0.226	4.36	1.36
0.940	0.189	0.187	5.03	1.88
0.958	0.168	0.166	5.74	2.32
0.945	0.149	0.148	6.40	2.81

TABLE II. Shock-Wave Compression Data for Heavy Mineral Oil

u mm/μsec	U mm/μsec	P kilobars	V/V_0
.0000	2.1856	.00	1.0000
.1000	2.3377	2.03	.9572
.2000	2.4897	4.33	.9196
.3000	2.6417	6.89	.8864
.4000	2.7937	9.72	.8568
.5000	2.9457	12.81	.8302
.6000	3.0977	16.17	.8063
.7000	3.2497	19.79	.7846
.8000	3.4018	23.67	.7648
.9000	3.5538	27.82	.7467
1.0000	3.7058	32.24	.7301
1.1000	3.8578	36.91	.7148
1.2000	4.0098	41.86	.7007
1.3000	4.1618	47.07	.6876
1.4000	4.3139	52.54	.6754
1.5000	4.4659	58.28	.6641
1.6000	4.6179	64.28	.6535
1.7000	4.7699	70.54	.6436
1.8000	4.9219	77.07	.6342
1.9000	5.0739	83.87	.6255
2.0000	5.2259	90.93	.6172
2.1000	5.3780	98.25	.6095
2.2000	5.5300	105.84	.6021
2.3000	5.6820	113.69	.5952
2.4000	5.8340	121.81	.5886
2.5000	5.9860	130.19	.5823
2.6000	6.1380	138.84	.5764
2.7000	6.2901	147.75	.5707
2.8000	6.4421	156.92	.5653
2.9000	6.5941	166.36	.5602
3.0000	6.7461	176.07	.5553

ACKNOWLEDGEMENT

The authors wish to thank Mr. George Hauver for advice and guidance during the course of the investigation.

REFERENCES

1. Bernard Hayes, "The Detonation Electric Effect," J. Appl. Phys., Vol 38, No. 2, February, 1967, pp 507-11.

2. Private communication from A. Melani, Ballistics Research Laboratories, Aberdeen Proving Ground, 1969.

3. White, heavy domestic mineral oil, Saybolt viscosity 335/350, density-0.87g/cc, Fisher Scientific Co. #0-120.

4. M. H. Rice, R. G. McQueen, and M. M. Walsh, "Compression of Solids by Strong Shock Waves," Solid State Physics, Vol 6, edited by Seitz and Turnbull, Academic Press Inc., New York and London, 1958.

5. Plexiglas type II UVA, density 1.18g/cc, Rohm and Haas, Philadelphia, Pa.

6. G. E. Hauver, and A. Melani, "Shock Compression of Plexiglas and Polystyrene." Aberdeen Proving Ground, Maryland, Ballistic Research Laboratories Report No. 1259, August, 1964.

7. G. E. Hauver, "The Dielectric Constant of Polyethylene Under Shock Compression" Aberdeen Proving Ground, Maryland, Ballistic Research Laboratories Report No. 1520, December, 1970.

8. Tektronix type 454.

9. F. E. Allison, "Thermodynamic States for Aluminum and Polystyrene" Aberdeen Proving Ground, Maryland, Ballistic Research Laboratories Report No. 1294, July, 1965.

10. M. Van Thiel, A. S. Kusubov, and A. C. Mitchell Eds., "Compendium of Shock Wave Data," University of California, Lawrence Radiation Laboratory, Livermore, California, UCRL 50108.

DISTRIBUTION LIST

No. of Copies	Organization
12	Commander Defense Documentation Center ATTN: TIPCR Cameron Station Alexandria, Virginia 22314
1	Director Advanced Research Projects Agency ATTN: Tech Info Department of Defense Washington, D.C. 20301
1	Commanding General U.S. Army Materiel Command ATTN: AMCDL Washington, D.C. 20315
1	Commanding General U.S. Army Materiel Command ATTN: AMCRD Dr. J. V. R. Kaufman Washington, D.C. 20315
1	Commanding General U.S. Army Materiel Command ATTN: AMCRD-BN, Mr. G. Burke Washington, D.C. 20315
1	Commanding General U.S. Army Materiel Command ATTN: AMCRD-BN-RE Mr. Corrigan Washington, D.C. 20315
1	Commanding General U.S. Army Materiel Command ATTN: AMCRD-TC, Mr. R. Rivkin Washington, D.C. 20315
1	Commanding General U.S. Army Materiel Command ATTN: AMCRD-TE Washington, D.C. 20315
1	Commanding General U.S. Army Materiel Command ATTN: AMCRD-TP Washington, D.C. 20315
1	Commanding General U.S. Army Aviation Systems Command ATTN: AMSAV-E 12th and Spruce Streets St. Louis, Missouri 63166
2	Commanding General U.S. Army Electronics Command ATTN: AMSEL-HL-CT Mr. S. Crossman AMSEL-CE Fort Monmouth, New Jersey 07703
2	Commanding General U.S. Army Missile Command ATTN: AMSMI-RBL AMSMI-R Redstone Arsenal, Alabama 35809
1	Commanding General U.S. Army Tank-Automotive Command ATTN: AMSTA-RHFL Warren, Michigan 48090
2	Commanding Officer U.S. Army Mobility Equipment Research and Development Center ATTN: Tech Docu Cen, Bldg 315 AMSME-RZT Fort Belvoir, Virginia 22060
1	Commanding General U.S. Army Munitions Command ATTN: AMSMU-RE Dover, New Jersey 07801

DISTRIBUTION LIST

No. of Copies	Organization
1	Commanding General U.S. Army Electronic Proving Ground ATTN: Tech Lib Fort Huachuca, Arizona 85613
1	Commanding General U.S. Army Weapons Command ATTN: AMSWE-RE Rock Island, Illinois 61202
1	Commanding General U.S. Army Safeguard Systems Command ATTN: SENSC, Mr. Davidson P.O. Box 1500 Huntsville, Alabama 35804
1	Director U.S. Army Safeguard Systems Office 1320 Wilson Blvd Arlington, Virginia 22209
1	Director U.S. Army Advanced Materiel Concepts Agency 2461 Eisenhower Avenue Alexandria, Virginia 22314
1	Director U.S. Army Air Mobility Research and Development Laboratory Ames Research Center Moffett Field, California 94035
1	Commanding Officer U.S. Army Harry Diamond Laboratories ATTN: AMXDO-TD/002 Washington, D.C. 20438
5	Commanding Officer U.S. Army Materials and Mechanics Research Center ATTN: AMXMR-T, Mr. J. Bluhm AMXMR-XH, Mr. J. Dignam AMXMR-XO, Mr. E. Hagge AMXMR-XP, Dr. J. Burke AMXMR-ATL Watertown, Massachusetts 02172
1	Commanding General U.S. Army Natick Laboratories ATTN: AMXRE, Dr. D. Sieling Natick, Massachusetts 01762
1	Deputy Assistant Secretary of the Army (R&D) Department of the Army Washington, D.C. 20310
1	HQ, DA(DACS-CW) Washington, D.C. 20310
1	HQ, DA(DARD-ARP) Washington, D.C. 20310
1	HQ, DA(DARD-MS) Washington, D.C. 20310
1	Commanding Officer U.S. Army Research Office (Durham) Box CM, Duke Station Durham, North Carolina 27706
1	Director U.S. Army Advanced Ballistics Missile Defense Agency ATTN: CRDABH-5, Mr. W. Loomis P.O. Box 1500 Huntsville, Alabama 35809

DISTRIBUTION LIST

No. of Copies	Organization
1	Commandant U.S. Army War College ATTN: Lib Carlisle Barracks Pennsylvania 17013
1	Commandant U.S. Army Command and General Staff College ATTN: Archives Fort Leavenworth, Kansas 66027
1	Mathematics Research Center U.S. Army University of Wisconsin Madison, Wisconsin 53706
3	Commander U.S. Naval Air Systems Command ATTN: AIR-604 Washington, D.C. 20360
3	Commander U.S. Naval Ordnance Systems Command ATTN: ORD-9132 Washington, D.C. 20360
1	Office of Naval Research ATTN: Code 402 Department of the Navy Washington, D.C. 20360
1	Commanding Officer and Director U.S. Navy Electronics Laboratory ATTN: Lib San Diego, California 92152
2	Director U.S. Naval Research Laboratory ATTN: Code 5270 Mr. F. MacDonald Code 2020, Tech Lib Washington, D.C. 20390
1	Commander U.S. Naval Weapons Laboratory ATTN: Code GR-9, Dr. W. Soper Dahlgren, Virginia 22448
1	AFATL (DLR) Eglin AFB Florida 32542
1	AFATL (DLRD) Eglin AFB Florida 32542
1	AFATL (DLRV) Eglin AFB Florida 32542
1	RADC (EMTLD, Lib) Griffiss AFB New York 13440
1	AUL (3T-AUL-60-118) Maxwell AFB Alabama 36112
1	AFML (Mr. J. Halpin) Wright-Patterson AFB Ohio 45433
1	Director Environmental Science Service Administration U.S. Department of Commerce Boulder, Colorado 80302

DISTRIBUTION LIST

No. of Copies	Organization
1	Director Jet Propulsion Laboratory ATTN: Lib (TDS) 4800 Oak Grove Drive Pasadena, California 91103
1	Director National Aeronautics and Space Administration Manned Spacecraft Center ATTN: Lib Houston, Texas 77058
1	Science and Technology Division Library of Congress Washington, D.C. 20540
2	President Research Analysis Corporation ATTN: Lib McLean, Virginia 22101
1	Dupont Experimental Laboratories ATTN: Mr. J. Lupton Wilmington, Delaware 19801
1	Sandia Laboratory Livermore Laboratory ATTN: Dr. S. Chiu P.O. Box 969 Livermore, California 94550
3	Sandia Corporation ATTN: Code 5133 Mr. L. Davison Div 1115 Dr. C. Harness Dr. D. Sutherland P.O. Box 5800 Albuquerque, New Mexico 87115
1	Willow Run Laboratories ATTN: Tech Docu Svcs P.O. Box 2008 Ann Arbor, Michigan 48104
5	Brown University Division of Engineering ATTN: Prof. R. Clifton Prof. H. Kolsky Prof. A. Pipkin Prof. P. Symonds Prof. J. Martin Providence, Rhode Island 02192
5	California Institute of Technology Division of Engineering and Applied Science ATTN: Dr. J. Miklowitz Dr. E. Sternberg Dr. J. Knowles Dr. T. Coguhey Dr. R. Shield Pasadena, California 91102
4	Carnegie Mellon University Department of Mathematics ATTN: Dr. D. Owen Dr. M. E. Gurtin Dr. B. Colerman Dr. W. Williams Pittsburgh, Pennsylvania 15213
1	Catholic University of America School of Engineering and Architecture ATTN: Prof. A. Durelli Washington, D.C. 20017

DISTRIBUTION LIST

No. of Copies	Organization
4	Cornell University Department of Theoretical and Applied Mechanics ATTN: Prof. E. Cranch Prof. G. Ludford Prof. D. Robinson Prof. Y-H Pao Ithaca, New York 14850
2	Forrestal Research Center Aeronautical Engineering Laboratory Princeton University ATTN: Dr. S. Lam Dr. A. Eringen Princeton, New Jersey 08540
1	Harvard University Division of Engineering and Applied Physics ATTN: Dr. G. Carrier Cambridge, Massachusetts 02138
2	Iowa State University Engineering Rsch Institute ATTN: Dr. A. Sedov Dr. G. A. Nariboli Ames, Iowa 50010
6	The Johns Hopkins University ATTN: Dr. J. Ericksen Dr. J. Bell Dr. R. Green Dr. C. Truesdell Dr. W. Hartman Dr. R. Pond 34th and Charles Streets Baltimore, Maryland 21218
3	Lehigh University Center for the Application of Mathematics ATTN: Dr. E. Varley Dr. R. Rivlin Prof. M. Mortell Bethlehem, Pennsylvania 18015
1	Massachusetts Institute of Technology ATTN: Dr. R. Probstein 77 Massachusetts Avenue Cambridge, Massachusetts 02139
1	Michigan State University College of Engineering ATTN: Prof. W. Sharpe East Lansing, Michigan 48823
1	New York University Department of Mathematics ATTN: Dr. J. Keller University Heights New York, New York 10053
1	North Carolina State University School of Engineering ATTN: Dr. T. SunChang Raleigh, North Carolina 27607
1	North Carolina State University Department of Engineering Mechanics ATTN: Dr. W. Bingham P.O. Box 5071 Raleigh, North Carolina 27607
3	Northwestern University The Technological Institute ATTN: Dr. G. Herrmann Dr. J. Achenbach Dr. S. Nemat-Nasser Evanston, Illinois 60201
2	Pennsylvania State University Engineering Mechanical Dept. ATTN: Prof. Jaunzemis Prof. N. Davids University Park, Pennsylvania 16802

DISTRIBUTION LIST

No. of Copies	Organization
1	Purdue University Institute for Mathematical Sciences ATTN: Dr. E. Caumberbatch Lafayette, Indiana 47907
2	Rice University ATTN: Dr. R. Bowen Dr. C. Wang P.O. Box 1892 Houston, Texas 77001
1	Southern Methodist University Solid Mechanics Division ATTN: Prof. H. Watson Dallas, Texas 75221
2	Southwest Research Institute Department of Mechanical Sciences ATTN: Dr. U. Lindholm Dr. W. Baker 8500 Culebra Road San Antonio, Texas 78228
1	Stanford Research Institute Poulter Laboratory 333 Ravenswood Avenue Menlo Park, California 94025
1	Tulane University Department of Mechanical Engineering ATTN: Dr. S. Cowin New Orleans, Louisiana 70112
2	University of California ATTN: Dr. M. Carroll Dr. P. Naghdi Berkeley, California 94704
1	University of California Department of Mechanics ATTN: Dr. R. Stern 504 Hilgard Avenue Los Angeles, California 90024
1	University of California Department of Aerospace and Mechanical Engineering Sciences ATTN: Dr. Y. C. Fung P.O. Box 109 La Jolla, California 92037
1	University of Delaware Department of Mechanical Engineering ATTN: Prof. J. Vinson Newark, Delaware 19711
3	University of Florida Department of Engineering, Science, and Mechanics ATTN: Dr. C. A. Sciammarilla Dr. L. Malvern Dr. E. Walsh Gainsville, Florida 32601
1	University of Houston Department of Mechanical Engineering ATTN: Dr. T. Wheeler Dr. R. Nachlinger Houston, Texas 77004
1	University of Illinois Department of Theoretical and Applied Mechanics ATTN: Dr. D. Carlson Urbana, Illinois 61801
1	University of Illinois at Chicago Circle College of Engineering Department of Materials Engineering ATTN: Prof. A. Schultz Box 4348 Chicago, Illinois 60680

DISTRIBUTION LIST

No. of Copies	Organization
1	University of Iowa ATTN: Dr. K. Valanis Iowa City, Iowa 50010
4	University of Kentucky Department of Engineering Mechanics ATTN: Dr. M. Beatty Prof. O. Dillon, Jr. Prof. P. Gillis Dr. D. Leigh Lexington, Kentucky 40506
1	The University of Maryland Department of Mechanical Engineering ATTN: Prof. J. Yang Dr. J. Dally College Park, Maryland 20742
1	University of Minnesota Department of Engineering Mechanics ATTN: Dr. R. Fosdick Minneapolis, Minnesota 55455
1	University of Notre Dame Department of Metallurgical Engineering and Materials Sciences ATTN: Dr. N. Fiore Notre Dame, Indiana 46556
1	University of Pennsylvania Towne School of Civil and Mechanical Engineering ATTN: Prof. Z. Hashin Philadelphia, Pennsylvania 19105
4	University of Texas Department of Engineering Mechanics ATTN: Prof. H. Calvit Dr. M. Stern Dr. M. Bedford Prof. Ripperger Austin, Texas 78712
1	University of Washington Department of Mechanical Engineering ATTN: Prof. J. Chalupnik Seattle, Washington 98105
2	Yale University ATTN: Dr. B. Chu Dr. E. Onat 400 Temple Street New Haven, Connecticut 96520
	Aberdeen Proving Ground
	Ch, Tech Lib Marine Corps Ln Ofc CDC Ln Ofc

UNCLASSIFIED
Security Classification

DOCUMENT CONTROL DATA - R & D

(Security classification of title, body of abstract and indexing annotation must be entered when the overall report is classified)

1. ORIGINATING ACTIVITY (Corporate author) USAARDC Ballistic Research Laboratories Aberdeen Proving Ground, Md.	2a. REPORT SECURITY CLASSIFICATION UNCLASSIFIED 2b. GROUP

3. REPORT TITLE

THE SHOCK HUGONIOT OF MINERAL OIL

4. DESCRIPTIVE NOTES (Type of report and inclusive dates)

5. AUTHOR(S) (First name, middle initial, last name)

Paul H. Netherwood

Daniel R. Tauber

6. REPORT DATE August 1972	7a. TOTAL NO. OF PAGES 33	7b. NO. OF REFS 10
8a. CONTRACT OR GRANT NO.	9a. ORIGINATOR'S REPORT NUMBER(S)	
b. PROJECT NO. 1T061102311A	BRL Memorandum Report No. 2214	
c.	9b. OTHER REPORT NO(S) (Any other numbers that may be assigned this report)	
d.		

10. DISTRIBUTION STATEMENT

Approved for public release; distribution unlimited.

11. SUPPLEMENTARY NOTES	12. SPONSORING MILITARY ACTIVITY Commanding General USA Materiel Command Washington, DC 20315

13. ABSTRACT

The shock Hugoniot of heavy mineral oil (density = 0.87g/cc) has been determined by plane shock wave experiments. A charged capacitor technique was used to measure shock velocities through specimens of mineral oil. Shock velocities through polymethyl methacrylate references specimens were measured by a shock-induced polarization technique, and impedance calculations were performed to establish the Hugoniot equation of state in mineral oil. Within the pressure range from 15 to 150 kilobars, the Hugoniot curve of heavy mineral oil was found to be represented by the linear relationship $U = 2.19 + 1.52u$, where U is shock velocity, u is particle velocity, and velocity units are mm/μsec.

DD FORM 1 NOV 68 1473 REPLACES DD FORM 1473, 1 JAN 64, WHICH IS OBSOLETE FOR ARMY USE.

UNCLASSIFIED
Security Classification

14. KEY WORDS	LINK A		LINK B		LINK C	
	ROLE	WT	ROLE	WT	ROLE	WT
Hugoniot, mineral oil, shock waves						